Amelioration of renal cortex histological alterations by aqueous garlic extract in gentamicin induced renal toxicity in albino rats: a histological and immunohistochemical study

Hala ZE Mohamed & Merry BK Shenouda

Taylor & Francis
Taylor & Francis Group

🔓 OPEN ACCESS ⟳ Check for updates

Amelioration of renal cortex histological alterations by aqueous garlic extract in gentamicin induced renal toxicity in albino rats: a histological and immunohistochemical study

Hala ZE Mohamed and Merry BK Shenouda (ID)

Department of Human Anatomy and Embryology, Faculty of Medicine, Assiut University, Assiut, Egypt

ABSTRACT

Background: Aminoglycosides, particularly gentamicin, endure crucial antibiotics in the armamentarium for severe Gram-negative bacterial infections through their significant risk for nephrotoxicity. Co-administration of several applicant nephroprotective agents has been investigated at the preclinical level. Garlic was proved to be an oxidative stress combatant with unique antioxidant potential.

Aim of the work: To assess renal cortex structural changes due to gentamicin treatment and the role of the aqueous garlic extract (AGE) in ameliorating these changes.

Material and methods: Thirty-two male albino rats were assigned into four equal groups. **Group I** (Control group) received 0.9% NaCl solution through oral gavage in the same volume as in AGE-treated group. **Group II** (AGE treated group) received AGE by oral gavage at 250 mg/kg/day. **Group III** (Gentamicin treated group) received Gentamicin at 80 mg/kg/day intraperitoneally. **Group IV** (Gentamicin and AGE cotreated group) received both gentamicin and AGE. The duration of the treatment was 21 days. Specimens of renal cortex of all groups were processed for light microscopic examination. Specimens were additionally prepared for electron microscopic examination. Morphometric study and statistical analysis were performed.

Results: Examination of the renal cortex in the gentamicin treated rats showed both proximal and distal tubular necrosis, vacuolation, desquamation and interstitial mononuclear cell infiltration. Masson's trichrome staining revealed intense deposition of collagen fibers. Strong positive immunoreaction for caspase-3 was observed. Ultrastructurally, the glomerulus showed thickened basement membrane, destructed endothelium. Proximal and distal convoluted tubular cells exhibited vacuolations, distorted mitochondria and nuclear chromatin condensation with loss of microvilli. AGE ameliorated these changes.

Conclusion: Aqueous garlic extract ameliorates the histological changes caused by gentamicin in the rat renal cortex.

1. Introduction

Aminoglycosides antibiotics are amongst the most widely used groups of antibiotics due to their low resistance, strong bactericidal action, and synergistic action with beta-lactam antibiotics. The most common members used in clinical practice are gentamicin and tobramycin [1]. Unfortunately, nephrotoxicity is the most eminent adverse effect related to aminoglycoside administration, Nevertheless, aminoglycoside nephrotoxicity can arise when serum levels are within the therapeutic range [2].

Megalin, a multiligand endocytic receptor, its activity is presumed to be a serious factor causing aminoglycoside-induced renal toxicity [3]. This receptor-mediated endocytosis is the cause for aminoglycoside accumulation in the lining cells of the renal tubules [4]. The tubular toxicity of gentamicin includes the death of epithelial cells with a significant inflammatory element and functional modification of the components of the cells responsible for transport processes of solute and water [5] and this was attributed mainly for oxidative stress [6].

The amelioration of nephrotoxicity caused by aminoglycosides has been tried by many researchers and several approaches have been proposed to reduce the this toxicity [4]. Performing a meta-analysis study, Vicente-Vicente et al. (2017) considered that antioxidants have displayed effectiveness at attenuating aminoglycoside renal toxicity in animal models, possibly because of their ability to impede many essential mechanisms concerned in renal cortex toxicity [7].

Garlic contains large amounts of antioxidants such as allicin, flavonoids and phenolics which are considered important phytochemicals [8]. Besides, Arreola et al. [9] indicated that garlic improves immunity as it stimulates lymphocytes, macrophages, eosinophils

and natural killer (NK) cells by regulation of phago-cytosis, cytokine secretion, immunoglobulin production, and macrophage activity. Its preparations are primarily liquid (oil, aqueous or solvent extracts) or solid (fresh cataplasm and dried garlic powder) [9].

The protective effect of garlic or its extracts in gentamicin-induced renal toxicity has not been fully explored yet. Though, some earlier studies showed that coadministration of garlic attenuates gentamicin-induced renal damage [10–12], most of those studies concentrated primarily on biochemical changes with no detailed account of the alterations in renal cortex structure, ultrastructure, or immunohistochemical expression of markers of apoptosis ensued due to gentamicin administration.

2. Aim of the work

The present research was performed to assess the possible ameliorative role of garlic as an antioxidant on the gentamicin-induced structural changes of the renal cortex in albino rats using histological, immunohistochemical and morphometric study.

3. Material and methods

3.1. Drugs

Gentamicin sulfate, existing as Epigent (80 mg/2 ml) ampoules was used in this experiment. It was manufactured by the Egyptian International Pharmaceutical Industries Company (EIPICO, Egypt).

3.2. Preparation of the aqueous garlic extract

It was prepared from the garlic cloves that were bought from the local market. They were peeled, washed and cut into small parts. Homogenization was done for 50 g in 75 ml cold sterile 0.9% NaCl. This mixture then was filtered three times. Centrifugation of the filtrate at 2000 rpm for 10 min was performed. The produced clear supernatant was completed by normal saline to 100 ml. Based on the weight of the initial material (50 g), the concentration of this garlic preparation was deliberated to be 500 mg/ml [13].

3.3. Experimental design and collection of samples

This study was carried out on 32 adult male albino rats of 190–250 g body weight. They were gained from the animal house, Faculty of Medicine, Assiut University. Rats were housed in stainless steel cages. The rats were kept under a 12 h light/dark cycle and supplied with food pellet diet and tap water ad libitum. They were randomly assigned into four equal groups: **Group I** (control group) received 0.9% NaCl solution through oral gavage in the same volume as in AGE-treated group. **Group II** (AGE-treated group) in which aqueous garlic extract was administered by oral gavage at a dose of 250 mg/kg/day [14]. **Group III** (Gentamicin treated group) received Gentamicin sulfate at a dose of 80 mg/kg/day daily by intraperitoneal injection. **Group IV** (Gentamicin and AGE cotreated group) received both aqueous garlic extract and gentamicin [15,16]. The duration of the treatments was 21 days [17]. All animal procedures conform the standard guidelines of animal ethics committee in Assiut University. At the end of the experiment, animals were anesthetized with ether, and a ventral abdominal incision was done to show the abdominal contents. The incision was extended superiorly to expose the thoracic contents. The left ventricle was then punctured, systemic vasculature perfusion was done for several minutes with 10% formalin solution.

3.4. For light microscopic examination

The kidneys were extracted, sliced and fixed in 10% formalin solution. The specimens were processed, embedded in paraffin. Specimens were cut at 5 micron thickness sections which were processed for staining with:

- Hematoxylin and eosin stain for demonstration of the structure of the renal cortex [18].
- Masson's trichrome stain for demonstration of collagen fibers deposition. [18].
- Immunohistochemical staining for Caspase-3 to detect apoptosis (Thermo Scientific, Fremont, California, USA).

For immunohistochemical staining, 5 μm thick paraffin sections were cut and placed on charged glass slides. The sections were deparaffinized and hydrated. Endogenous peroxidase activity was blocked by embedding in 10% hydrogen peroxide for 10 min. Sections were put in 0.01 mol/l citrate buffer (pH = 6) for 5 min in the microwave for antigen retrieval. To prevent the nonspecific staining of the background, washing of the slides in PBS at pH 7.4 was done and then they were incubated in 1% BSA dissolved in PBS for 30 min at 37° C. Two drops of ready-to-use caspase-3 (CPP32) Ab-4 rabbit polyclonal antibody were put on the sections, excluding the negative controls, and they were incubated overnight at room temperature. The slides were washed with PBS then a few drops of biotinylated goat-polyvalent secondary antibody were applied for 10 min. The slides then were incubated DAB solution for 15 minutes, counterstained by Mayer's hematoxylin, dehydrated and mounted [19].

3.5. For electron microscopic examination

Renal cortex tissue was cut into 1 mm^3 pieces and fixed in 2.5% buffered glutaraldehyde for 24 hours. These were washed in three changes of cacodylate buffer (pH 7.2) for 20 minutes in each change. Specimens were postfixed in osmium tetroxide. Dehydration of specimens was done using ascending grades of ethyl alcohol. Embedding was accomplished in Epon 812. Semithin sections of 1 μm in thickness were cut, stained with toluidine blue, examined and photographed. From selected regions, ultrathin sections were cut at 50–80 nm in thickness and were placed on copper grids. They were stained using uranyl acetate and lead citrate. They were examined by transmission electron microscopy (Jeol- JEM- 100 CXII; Jeol, Tokyo, Japan) and photographed in the Assiut University Electron Microscopy Unit [20].

3.6. Morphometric study

Measurements were quantified in five non-overlapping fields images in ten sections that were randomly chosen in three different rats from each group. Images were measured by Image J software (version1.52, Public Domain) at x400 magnification. The following were measured:

(1) -The mean area percentage of collagen fibers deposition in sections stained by Masson's trichrome [21].
(2) The mean area percentage of caspase –3 immunostaining. The areas show brown immunostaining were selected for estimation irrespective of staining intensity [22].

3.7. Statistical analysis

The data were expressed as the mean ± standard error of mean. Statistical analysis was performed using Statistical Package for the Social Sciences software (SPSS 16.0 Inc, Chicago. USA), using one-way analysis of variance (ANOVA) followed by post-hoc Tukey's test. Statistical significance was established at the value of $p < 0.05$.

4. Results

Histological examination of both the control and AGE-treated groups showed identical normal structure of the renal cortex. Figures for the control group were demonstrative for both groups.

4.1. Light microscopic results

Examination of the hematoxylin and eosin-stained sections of the renal cortex in the control group revealed that renal corpuscle consisted of the Bowman's capsule surrounding the glomerulus, the parietal layer of which was lined by a layer of flat epithelium. The renal space separated the glomerulus from the parietal layer of the Bowman's capsule. Proximal-convoluted tubules appeared with small uneven lumen lined by a layer of cuboidal cells with granular cytoplasm and rounded basal nuclei. Distal convoluted tubules showed wider lumen with pale cuboidal cells with central rounded nuclei (Figure 1 (A)). In gentamicin treated group distorted architecture of the renal cortex was observed. Empty spaces were observed. Many renal corpuscles showed shrinkage with dilated renal spaces. The lining cells of the proximal and distal convoluted tubules displayed marked vacuolated cytoplasm and pyknotic nuclei. Desquamated cells could be seen in the tubular lumen. Some areas showed mononuclear cellular infiltration (Figure 1(B)). In gentamicin and AGE cotreated rats, renal corpuscle appeared nearly normal with mild focal injury of the proximal and distal convoluted tubules (Figure 1(C)).

Masson's Trichrome stain in the control group demonstrated little collagen deposition within the
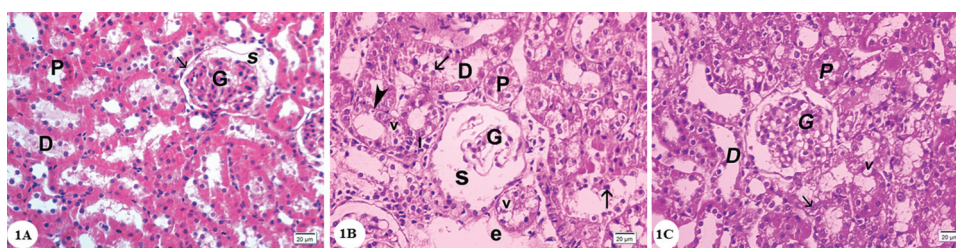
Figure 1. Photomicrographs of the renal cortex sections stained by hematoxylin and eosin: (A) **Control group** showing renal corpuscle with glomerulus (G), the parietal layer of Bowman's capsule consists of a layer of flat cells (arrow), Bowman's space(S). The proximal convoluted tubules (P) with cuboidal cells lining, narrow lumen and deeply stained cytoplasm. Distal convoluted tubules (D) with a wider lumen, cuboidal cells, rounded central nuclei and the cytoplasm is pale. (B) **Gentamicin treated group** showing shrunken glomerulus (G) and dilated renal space(S). Cells of both proximal (P) and distal (D) convoluted tubules showing vacuolated cytoplasm (v), most of them with pyknotic nuclei (arrowhead). Desquamated cells can be observed in the tubular lumen (arrows). Note the presence of empty spaces(e)and mononuclear cellular infilteration (I). **(C) Gentamicin and AGE cotreated group** showing apparently normal renal cortex,glomerulus(G), some cells show vacuolations of cytoplasm (v) most of the cells have vesicular nuclei (arrows). (Hx & E x400).
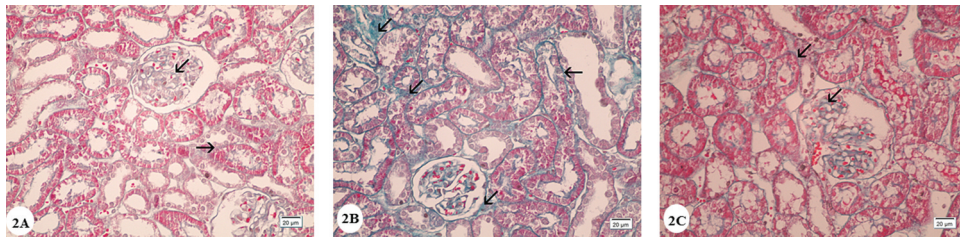
Figure 2. Photomicrographs of Masson's Trichrome stained renal cortex sections: (A) **Control group** showing minimal collagen fiber deposition in the renal corpuscles and in between renal tubules (arrows). (B) **Gentamicin treated group** showing intense collagen fiber deposition in the renal corpuscles and in between proximal and distal convoluted tubules (arrows). (C) **Gentamicin and AGE cotreated group** showing little collagen fiber deposition in the renal corpuscles and in between renal tubules (arrows). (Masson's Trichrome x 400).

interstitium with no fibrotic lesions (Figure 2(A)). In the renal cortex of the gentamicin treated group, Masson's trichrome staining revealed intense deposition of collagen fibers within the glomerular basement membrane, around Bowman's capsule and in the interstitial tissue between the renal tubules (Figure 2 (B)). Examination of the Masson's trichrome stained sections of the gentamicin and AGE cotreated group showed mild collagen fibers deposition (Figure 2(C)).

Semithin sections of the renal cortex of the control group stained with toluidine blue showed that the renal corpuscle consisted of a glomerular capillaries that were surrounded by Bowman's capsule. Parietal layer of Bowman's capsule was lined with flattened cells and podocytes which was investing the glomerular capillaries form the visceral layer. Podocytes had pale nuclei and pale stained cytoplasm. Mesangial cells could be recognized by their darkly stained nuclei and the deeply stained matrix surrounded them among the glomerular capillaries (Figure 3(A)). Proximal convoluted tubules were lined with cuboidal cells and with noticeable apical brush border besides prominent basal striations. The nuclei appeared central, vesicular with prominent nucleoli. Distal convoluted tubules cells appeared to lack apical brush border and had vesicular nuclei and pale cytoplasm (Figure 4(A)).

In gentamicin treated group, semithin sections of the renal cortex showed that glomeruli had congested capillaries and hyperplasia of mesangial cells in addition to thickening of the parietal layer of Bowman's capsule. Some glomeruli were destructed (Figure 3(B)). Most of cells in proximal convoluted tubules exhibited multiple cytoplasmic vacuoles, loss of brush border as well as enlarged lysosomes, that seemed as small cellular inclusions that were darkly stained rounded or irregular bodies (Figure 4(B)). The lining cells of the distal tubules showed the presence of vacuolated cytoplasm, many lysosomes and pyknotic nuclei. Some tubules showed severely injured lining cells and desquamating cells leaving basement membrane with denuded places (Figure 4(C)).

In gentamicin and AGE cotreated group preservation of renal corpuscle structure with nearly normal glomerulus was observed (Figure 3(C)). Most of the cells lining of the proximal and distal convoluted tubules have rounded vesicular nuclei. In addition, preservation of the brush border was observed. Some cells with vacuolated cytoplasm were noticed (Figure 4(D)).

4.2. Immunohistochemical results

Immunohistochemical staining of the renal cortex of control rats using anti caspase-3 revealed negative caspase-3 reaction in the cytoplasm of the cells of convoluted tubules (Figure 5(A)). Immunohistochemical staining of the renal cortex of gentamicin treated group using anti caspase-3 showed greatly expressed
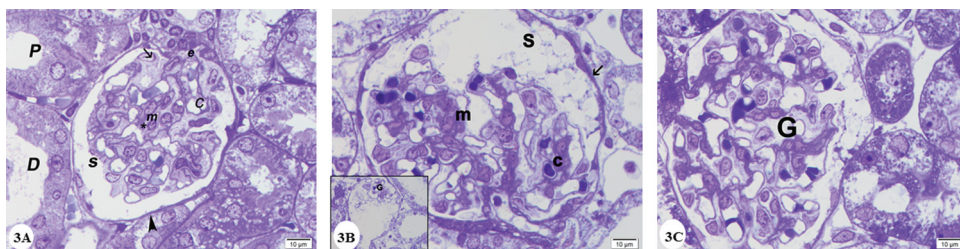
Figure 3. Photomicrographs of semithin sections of the renal cortex: (A) **Control group** showing lining endothelium(e) of glomerular capillaries (C) invested by podocytes with pale stained cytoplasm and nuclei (arrow), mesangial cells(m)surrounded by deeply stained mesangial matrix (*). Note the renal space (s) between parietal (arrowhead) and visceral layers of Bowman's capsule, (P) Proximal and (D) distal convoluted tubules. (B) **Gentamicin treated group** showing hyperplasia of mesangial cells (m), congested capillaries(c) and thickening of the parietal layer of Bowman's capsule (arrow). Inset showing destructed renal glomerulus (G). (C) **Gentamicin and AGE cotreated group** showing preservation of renal corpuscle structure with nearly normal glomerulus(G). (Toluidine blue x1000).
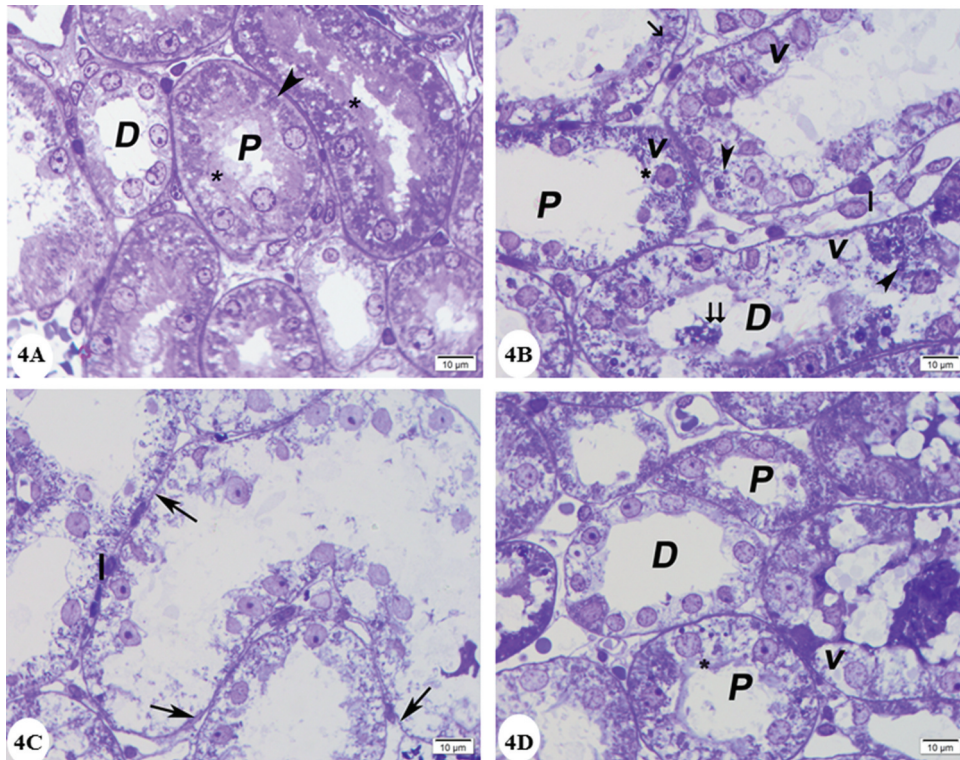
Figure 4. Photomicrographs of renal cortex semithin sections: (A) **Control group** showing lining cells of proximal convoluted tubules (P) which are cuboidal and have rounded vesicular nuclei, apical prominent brush borders (*) and clear basal striations (arrowhead). Distal convoluted tubules (D) have cuboidal cell lining with rounded nuclei and paler cytoplasm. (B) and (C) **Gentamicin treated group:(B)** showing that the lining cells of proximal (P) and distal (D) convoluted tubules with vacuolated cytoplasm (v), many deeply stained lysosomes (arrow heads) pyknotic nuclei (arrow) marked loss of brush border (*). Desquamated cells in the lumen (double arrow) are noticed. Note interstitial cellular infiltrate (I). (C) showing loss of lining cells of some tubules (arrow). (D) **Gentamicin and AGE cotreated group** showing that most of the cells lining proximal convoluted tubules (P) and distal convoluted tubules (D) have rounded vesicular nuclei. Brush border is preserved (*) Some cells have vacuolated cytoplasm(v). (Toluidine blue x1000).
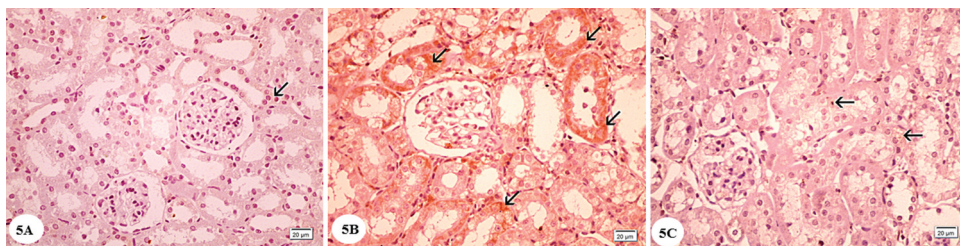
Figure 5. Photomicrographs of immunohistochemically stained sections for caspase −3 of the renal cortex: (A) **Control group** showing negative cytoplasmic reactions for caspase-3 in the cells of renal tubules (arrow) (B) **Gentamicin treated group** showing widespread cytoplasmic immunoreactivity reactions for caspase-3 (arrows). (C) **Gentamicin and AGE cotreated group** showing weak cytoplasmic reactions for caspase-3 (arrow). (caspase-3 immunostaining x400).

cytoplasmic caspase-3 reaction in both the proximal and distal convoluted tubules (Figure 5(B)). In gentamicin and AGE cotreated group immunohistochemical staining using anti caspase-3 presented slightly expressed caspase-3 reaction in the tubular cells' cytoplasm (Figure 5(C)).

4.3. Transmission electron microscopic results

Examination of the ultrastructure of the glomerulus in the control group showed the presence of glomerular capillary loops lined by fenestrated endothelium. They are surrounded by podocytes which had irregular nuclei. Primary and secondary processes could be observed extend from the cell body of podocytes. The secondary processes appeared in contact with the outer surface of the glomerular basement membrane. The glomerular basement membrane appeared with regular thickness and consisted of central electron-dense lamina densa and on both sides of which electron lucent lamina rara. Mesangial cells surrounded by mesangial matrix were noticed (Figure 6
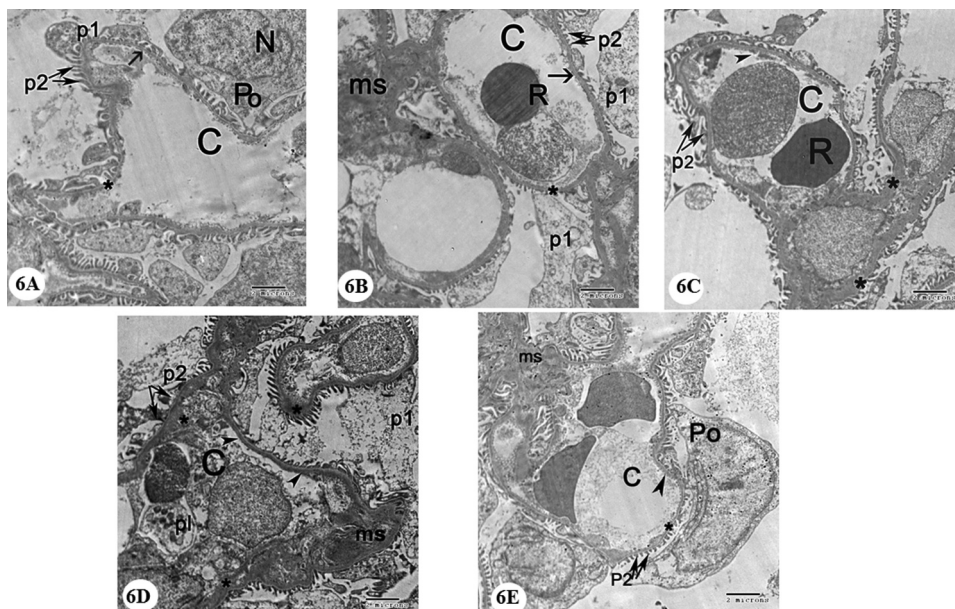
Figure 6. Electron micrographs of a portion of renal corpuscle: (A) and (B) **Control group** showing capillary in the glomerulus (C) with fenestrated endothelium lining (arrow) with uniform lamina densa bordered on each side with lamina rara (*), red blood cell (R). Podocyte cell (Po) with folded nucleus(N) gives primary process (p1) and numerous secondary processes (p2) separated by filtration slits. Note mesangial cell surrounded by mesangial matrix (ms). (C) and (D) **Gentamicin treated group** showing the capillary in a glomerulus (C) that is lined with distorted endothelium (arrow heads) with irregular thickening of the basement membrane (*), distorted secondary processes of podocytes (p2). Note electron dense mesangial matrix (ms). (E) **Gentamicin and AGE cotreated group** demonstrating glomerular capillary (C) with fenestrated endothelium (arrowhead). Note the presence of more or less normal basement membrane structure (*) and secondary processes of podocytes (p2) separated by filtration slits, podocyte (Po) and mesangial matrix (ms). (x 4800).
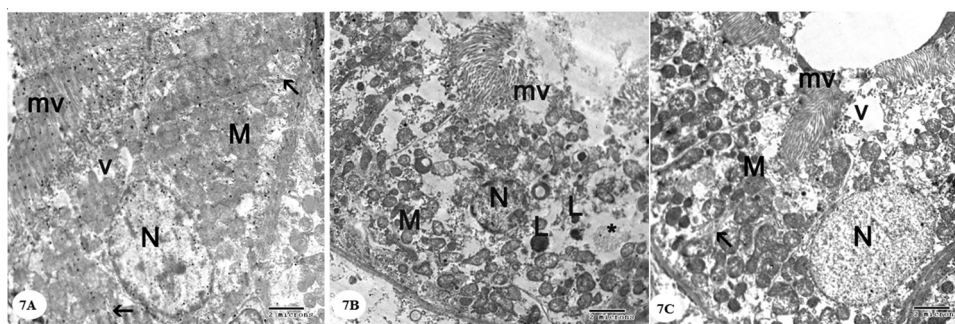
Figure 7. Electron micrographs of a portion of the proximal convoluted tubule: (A) **Control group** showing that the cell has an euchromatic nucleus (N) with prominent nucleolus, basal infoldings of the cell (arrow) with longitudinally arranged mitochondria (M), apical microvilli (mv), and apical vacuoles (v). (B) **Gentamicin treated group** showing the cell has a small condensed nucleus (N), loss of basal infoldings, mitochondria (M) with distorted cristae and matrix loss, loss of apical microvilli (mv), the cytoplasm shows the presence of many lysosomes (L) and vacuoles(*). (C) **Gentamicin and AGE cotreated group** showing that the cell has an euchromatic nucleus (N) with, basal infoldings of the cell (arrow) with mitochondria(M), apical microvilli (mv) and some vacuoles(v) can be noticed (x 4800).

(A)). Examination of the cells of the proximal convoluted tubules showed the presence of rounded euchromatic nucleus with prominent nucleolus. The cells showed basal infoldings of the cytoplasm with numerous mitochondria appeared longitudinally arranged. Microvilli could be clearly observed on the luminal surface of the cells of the proximal convoluted tubule (Figure 7(A)). The cell of the distal convoluted tubules showed the presence of euchromatic rounded central nucleus, many mitochondria and few apical blunt microvilli (Figure 8(A)).

Examination of the glomerulus in gentamicin treated group showed that the glomerular basement membrane showed areas of thickening. Degenerated endothelium could be identified. Secondary processes of podocytes were seen vacuolated and disrupted with electron-dense mesangial matrix around mesangial cells (Figure 6(B)).

The cells of proximal convoluted tubules in gentamicin treated rats showed vacuolated cytoplasm, mitochondria were seen with distorted cristae and matrix loss. loss of microvilli. The nucleus appeared small and
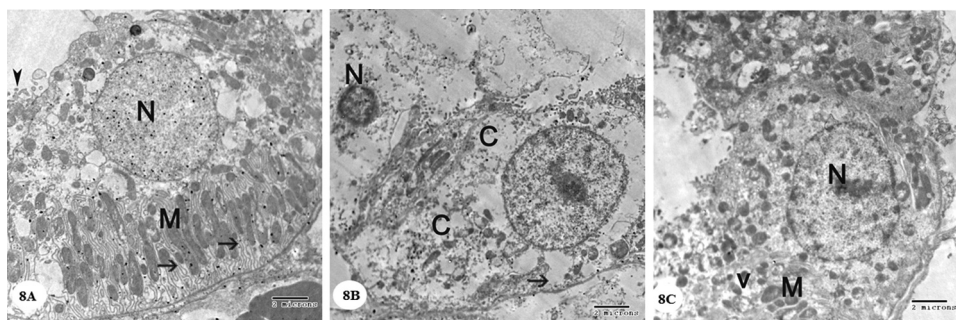
Figure 8. Electron micrographs of a portion of the distal convoluted tubule: (A) **Control group** showing that the cell has an euchromatic nucleus (N), basal infoldings of the cell (arrows) with longitudinally arranged mitochondria (M), few apical blunt microvilli (arrowhead). (B) **Gentamicin treated group** showing that the cell has condensed nucleus (N), the cytoplasm(c) appears rarified with many vacuoles and loss of basal infoldings (arrow) and most of cytoplasmic organelles. . (C) **Gentamicin and AGE cotreated group** showing that the cell has an euchromatic nucleus (N), mitochondria (M) and some vacuoles(v) in the cytoplasm could be seen. (x 4800).

showed condensation of chromatin (Figure 7(B)). Cells of the distal convoluted tubules appeared with vacuolated cytoplasm and destructed organelles. The nucleus was shrunk with condensed chromatin (Figure 8(B)).

Renal cortex in gentamicin and AGE cotreated rats showed mild glomerular changes (Figure 6(C)). The cells of proximal convoluted tubules showed rather distortion of the basal infoldings with euchromatic nucleus (Figure 7(C)). The cells of distal convoluted tubules appeared nearly like the control (Figure 8(C)).

4.4. Morphometric results

The mean area percentage of collagen fibers deposition in the renal cortex in group III (gentamicin treated group) was increased significantly in comparison with group I (control group) and group II (AGE treated group). In group IV (gentamicin and AGE cotreated group), the mean area percentage of collagen fibers deposition was significantly decreased compared to group III (gentamicin treated group) (p < 0.05) (Table 1).

Concerning the statistical analysis of the area percentage of caspase-3 immunostaining in the renal cortex in different experimental groups, a significant increase in group III (gentamicin treated group) in comparison with group I (control) and group II

(AGE-treated group) was noticed. Area percentage of caspase-3 immunostaining of the renal cortex showed significant decrease in group IV (gentamicin and AGE cotreated group) in comparison to group III (gentamicin treated group) (p < 0.05) (Table 2).

5. Discussion

One of the most imperative side effects and limitations of the use of aminoglycoside antibiotics, particularly gentamicin, is nephrotoxicity [5]. Additionally, because of increasing numbers of widespread chronic kidney diseases patients, scientists are challenged with finding new protecting approaches for this medical problem [23]. In the present study administration of gentamicin for 21 day was to produce a model of gentamicin-induced chronic renal failure [17].

The results of the present study showed that rat renal cortex after administration of gentamicin for 21 days showed marked destructive lesions in the form of shrinkage of renal corpuscles with dilated renal spaces. These results confirm the findings of Mahmoud et al [24] who noticed complete atrophy of some glomeruli and shrinkage of glomerular capillaries in other glomeruli in gentamicin treated rats. Regarding the cells of the proximal and distal convoluted tubules this study showed marked vacuolated cytoplasm and pyknotic nuclei.

Table 1. Showing the mean area percentage ± SE of collagen fibers deposition in all experimental groups(n = 5).

Groups	Group I	Group II	Group III	Group IV
Mean area % of collagen fibers	8.04 ± 0.39	7.72 ± 0.22	21.14 ± 0.69*	11.40 ± 0.51#

Data are presented as means± SE. n = 5
P = 0.00
* significant increase in comparison with Group I and II
# significant decrease in comparison with Group III

Table 2. Showing the mean area percentage ±SE of caspase-3 immunostaining in all experimental groups(n = 5).

Groups	Group I	Group II	Group III	Group IV
Mean area % of caspase-3 immunostaining	0.74 ± 0.039	0.57 ± 0.06	23.75 ± 0.27*	3.84 ± 0.50#

p=0.00* Significant increase in comparison with Group I and II
# Significant decrease in comparison with Group III

Desquamated cells could be seen in the tubular lumen. This was consistent with Veljković et al. [25] who noticed that proximal convoluted tubules showed necrosis, vacuolation of cytoplasm and epithelial desquamation after gentamicin treatment. Taken into consideration that in this work cells of both proximal and distal convoluted tubules are affected. However, it was reported that distal tubules are significantly less affected by cytotoxic effects of gentamicin [26]. In our experiment this finding was interpreted by the study of Toubeau et al. [27] who stated that gentamicin could access the distal tubules with longer treatment period.

Some areas of the renal cortex showed mononuclear cellular infiltration which was compatible with Katary and Salahuddin [28] who investigated the important role of the inflammation in gentamicin-induced renal injury and signified the elevated levels of inflammatory cytokines IL-6 and TNF-α besides their mRNA synthesis. Gentamicin is known to greatly reduce the level of NF-κB inhibitor (IkB-α) protein resulting in stimulation of inflammatory cytokines; TNF- α and IL-6 synthesis [29]. By the same token, gentamicin treatment leads to an increase in macrophage infiltration and stimulates secretion of IL-6 by macrophages which in turn regulates inflammatory and immune responses [30].

Empty spaces were observed in hematoxylin and eosin sections and these was in accordance with El-Safti and Mohammed [31] who clearly observed multiple diffuse empty spaces in the renal cortex in adenine-induced chronic renal failure model.

In the present research examination of the semithin sections in gentamicin treated group revealed the presence of many enlarged lysosomes, this was consistent with Toubeau et al. [32] who recognized the presence of enlarged irregular lysosomes in examination of semithin sections of renal cortex of rats treated with amikacin. This can be accounted for by the fact that gentamicin results in a condition called lysosomal phospholipidosis. This rsults from an interaction between the membrane anionic phospholipid and the cationic aminoglycoside which is the initial phase for the development of gentamicin cytotoxicity. As a result, the lysosomes release their hydrolytic enzymes as they function improperly. This is closely linked to cell death [33,34].

Masson's trichrome stain in this work was used to asses fibrosis. Sections from the gentamicin treated group disclosed statistically significant increased deposition of collagen fibers between renal tubules and within the glomeruli. This agreed with Aldahmash et al. [35] who reported intense collagen fibers deposition in glomeruli and in between cortical tubules in gentamicin-treated mice. Renal interstitial fibrosis is promoted by a diversity of inflammatory cells and growth factors as transforming growth factor-beta 1 (TGF-β1), produced mainly by macrophages. It plays a significant role in the induction of resident myofibroblasts responsible to produce extracellular matrices, such as collagen and fibronectin [36,37]. From the standpoint of increased levels of tumor necrosis factor-α, due to gentamicin treatment, it has a role in production of myofibroblasts by the conversion of interstitial cells with ensuing collagen deposition [38].

This study revealed the presence of statistically significant increased immunohistochemical expression of apoptotic protein caspase-3, in the renal cortex of gentamicin treated rats this was in accordance with Suh et al. [39] who confirmed a marked increase in expression of caspase-3 protein in the kidneys treated with gentamicin. Activation of caspase was proved to be one of the features of apoptosis induced by gentamicin [40]. Casanova et al. [6] explained that the hierarchy of structural mechanisms underlying the development of aminoglycoside renal toxicity induced chiefly by oxidative stress.

Ultrastructurally, the glomerular basement membrane showed areas of thickening. These results were consistent with Stojiljkovic et al. [41] who reported that the glomerular basement membrane was significantly thickened in gentamicin-treated rats. Degenerated endothelial cells could be identified. Secondary processes of podocytes were seen vacuolated and disrupted in addition to electron-dense mesangial matrix around mesangial cells. This study confirmed the findings of Abdelsameea, et al. [42] who encountered that gentamicin caused several diverse changes in the ultrastructure of the renal cortex in the form of disordered blood renal barrier that was associated with degenerated endothelium, vacuolated podocytes, dense mesangial matrix and thickened basement membrane

In this study, cells of both proximal and convoluted tubules showed vacuolated cytoplasm, in addition to loss of microvilli. These were in agreement with Kohn et al. [43] and Mahmoud [44] who reported that the cells of the proximal convoluted tubules after gentamicin treatment seemed degenerated that was demonstrated by vacuolization of the cytoplasm, myeloid body and lysosomal accumulation, mitochondrial alterations, and loss of both microvilli and basal infoldings.

Mitochondrial alterations were observed in the form of distorted cristae and matrix loss. These harmonized with Galal et al. [22] who reported the presence of vacuolated swollen mitochondria with loss of cristae partially or completely which was correlated to oxidative stress. These alterations in mitochondria known to be an early indicator of apoptosis and an adaptive process to an unfavorable environment due to the excessive cellular exposure to free radicals [45].

Garlic has two main components, definitely flavonoids and sulfur-containing compounds (allyl-cysteine, diallyl sulfide and trisulfide). These compounds play a significant role in the extensively established antioxidant, hypolipidemic, hypocholesterolemic, antitumor and immunomodulatory activities of garlic [46].

The results of the present work revealed that administration of aqueous garlic extract with gentamicin revealed that renal tubules and renal corpuscles showed more or less normal structure with few tubules affected. Ultrastructurally the endothelial lining, secondary processes of podocytes and the lining cells of the convoluted tubules displayed amelioration in structural changes when compared with that treated only with gentamicin. These results confirmed the findings of Pedraza-Chaverri et al. (2000) who assessed the protective effect of garlic against gentamicin nephrotoxicity and documented that it prevents the increase in lipoperoxidation and the reduction in the antioxidant enzymes activity detected in renal cortex of rats treated with gentamicin [10].

Masson's trichrome staining showed significant decrease in collagen fibers deposition in the interstitium and this was in agreement with Gedik et al. [47] who suggested that aqueous garlic extract has a protective effect against hepatic fibrosis by reducing formation and deposition of extracellular matrix constituents induced by inflammation. This is because garlic downregulates proinflammatory cytokines including IL-6, IL-2 and TNF-α, by T cells and inhibits proinflammatory response signaling [48].

The antiapoptotic effect of aqueous garlic extract was investigated in this work. Immunohistochemical examination of renal cortex using apoptotic protein, caspase-3 antibody showed that aqueous garlic extract administration with gentamicin significantly decreased the expression of caspase-3 in comparison with the gentamicin group. This was confirmed statistically. This was in agreement with Galal et al. [22] who revealed that co-administration of garlic reduced the high levels of caspase-3 provoked by lead administration in cerebrum and cerebellum in rats. This was explained by the presence of about 200 chemical compounds in garlic as sulfur-containing allicin, ajone, allin, peroxidase, myrosinase and allinase [49]. Galal and Abd El-Rady [50,51] reported that AGE restores the normal balance between oxidants and antioxidants in renal tissue when administered with gentamicin and this was attributed to its potent antioxidant activity.

The present findings suggest that AGE at a dose of 250 mg/kg/day can ameliorate the structural damage results from administration of gentamicin in albino rats. We suggest that this occur through the antioxidant and antiapoptotic activity of garlic.

Disclosure statement

There are no conflicts of interest.

ORCID

Merry BK Shenouda http://orcid.org/0000-0002-7192-6463

References

[1] McWilliam SJ, Antoine DJ, Smyth RL, et al. Aminoglycoside-induced nephrotoxicity in children. Pediatr Nephrol. 2017;32(11):2015–2025.

[2] Decker BS, Molitoris BA. Aminoglycoside-induced nephrotoxicity. Compr Toxicol Third Ed. 2017;14–15(6):256–273.

[3] Schmitz C, Hilpert J, Jacobsen C, et al. Megalin deficiency offers protection from renal aminoglycoside accumulation. J Biol Chem. 2002;277(1):618–622.

[4] Watanabe A, Nagai J, Adachi Y, et al. Targeted prevention of renal accumulation and toxicity of gentamicin by aminoglycoside binding receptor antagonists. J Control Release. 2004;95(3):423–433.

[5] Lopez-Novoa JM, Quiros Y, Vicente L, et al. New insights into the mechanism of aminoglycoside nephrotoxicity: an integrative point of view. Kidney Int. 2011;79(1):33–45.

[6] Casanova AG, Vicente-Vicente L, Hernández-Sánchez MT, et al. Key role of oxidative stress in animal models of aminoglycoside nephrotoxicity revealed by a systematic analysis of the antioxidant-to-nephroprotective correlation. Toxicology. 2017;385(April):10–17.

[7] Vicente-Vicente L, Casanova AG, Hernández-Sánchez MT, et al. A systematic meta-analysis on the efficacy of pre-clinically tested nephroprotectants at preventing aminoglycoside nephrotoxicity. Toxicology. 2017;377:14–24.

[8] Lanzotti V. The analysis of onion and garlic. J Chromatogr A. 2006;1112(1–2):3–22.

[9] Arreola R, Quintero-fabián S, López-roa RI, et al. Immunomodulation and anti-inflammatory effects of garlic compounds. J Immunol Res. 2015;2015:401630.

[10] Pedraza-Chaverrí J, Maldonado PD, Medina-Campos ON, et al. Garlic ameliorates gentamicin nephrotoxicity : relation to antioxidant enzymes. Free Radic Biol Med. 2000;29(7):602–611.

[11] Maldonado PD, Barrera D, Medina-campos ON. Aged garlic extract attenuates gentamicin induced renal damage and oxidative stress in rats. Life Sci. 2003;73(20):2543–2556.

[12] El-Kashef DH, El-Kenawi AE, Suddek GM, et al. Protective effect of allicin against gentamicin-induced nephrotoxicity in rats. Int Immunopharmacol [Internet]. 2015;29(2):679–686. .

[13] Nwokocha CR, Ozolua RI, Owu DU, et al. Antihypertensive properties of Allium sativum (garlic) on normotensive and two kidney one clip hypertensive rats. Niger J Physiol Sci. 2011;26(2):213–218.

[14] Becerra-Torres SL, Soria-Fregozoa C, Jaramillo-Juárezb F, et al. Allium sativum aqueous extract prevents potassium dichromate-induced nephrotoxicity and lipid oxidation in rats. J Pharm Pharmacogn Res. 2014;2(2):45–52.

[15] Boroushaki MT, Asadpour E, Sadeghnia HR, et al. Effect of pomegranate seed oil against gentamicin - induced nephrotoxicity in rat. J Food Sci Technol. 2014;51(11):3510–3514.

[16] Reimschuessel R, Williams D. Development of new nephrons in adult kidneys following gentamicin-induced nephrotoxicity. Ren Fail. 1995;17(2):101–106.

[17] Gomaa A, Abdelhafez AT, Aamer HA. Garlic (Allium sativum) exhibits a cardioprotective effect in

experimental chronic renal failure rat model by reducing oxidative stress and controlling cardiac Na$^+$/K$^+$-ATPase activity and Ca^{2+} levels. Cell Stress Chaperones. 2018;23(5):913–920.

[18] Drury R, Wallington E. Carleton's histological technique. 5th ed. New York and Toronto: Oxford University Press; 1980. p. 183–184.

[19] Sanderson S, Wild G, Cull AM, et al. Immunohistochemical and immunofluorescent techniques. In: Suvarna SK, Layton C, Bancroft JD, editors. Bancroft's Theory and Practice of Histological Techniques. Eighth ed. Elsevier Limited, China; 2019. p. 337–394.

[20] Hayat MA. Principles and techniques of electron microscopy: biological applications. 4th ed. Cambridge, UK: Cambridge University Press; 2000. p. 35–59.

[21] Altayeb Z, Salem M. Light and electron microscopic study on the effect of immobilization stress on adrenal cortex of adult rats and possible ameliorative role of vitamin E. J Med Histol. 2017;1(1):44–56.

[22] Galal MK, Elleithy EMM, Abdrabou MI, et al. Modulation of caspase-3 gene expression and protective effects of garlic and spirulina against CNS neurotoxicity induced by lead exposure in male rats. NeuroToxicology. 2019;72(November 2018):15–28.

[23] Thomas R, Kanso A, Sedor JR. Chronic kidney disease and its complications. Prim Care. 2008;35(2):329–vii.

[24] Mahmoud AM, Ahmed OM, Galaly SR. Thymoquinone and curcumin attenuate gentamicininduced renal oxidative stress, inflammation and apoptosis in rats. Excli J. 2014;13:98–110.

[25] Veljković M, Stojiljković N, Pavlović DR, et al. Morphological and morphometric study of protective effect of green tea in gentamicin-induced nephrotoxicity in rats. Life Sci. 2016;147:85–91.

[26] Fujiwara K, Shin M, Matsunaga H, et al. Light-microscopic immunocytochemistry for gentami- cin and its use for studying uptake of the drug in kid- ney. Antimicrob Agents Chemother. 2009;53(8):3302–3307.

[27] Toubeau G, Maldague P, Heuson-Stiennon JA, et al. Morphological alterations in distal and collecting tubules of the rat renal cortex after aminoglycoside administration at low doses. Virchows Arch B Cell Pathol Incl Mol Pathol. 2008;51(1):475–485.

[28] Katary M, Salahuddin A. Ameliorative effect of gossypin against gentamicin-induced nephrotoxicity in rats. Life Sci [[Internet]]. 2017;176:75–81.

[29] Anandan R, Subramanian P. Renal protective effect of hesperidin on gentamicin induced acute nephrotoxicity in male Wistar albino rats. Redox Rep. 2012;17:219–226.

[30] Fielding CA, McLoughlin RM, McLeod L, et al. IL-6 regulates neutrophil trafficking during S.A. acute inflammation via STAT3. J Immunol. 2008;181 (3):2189–2195.

[31] El-Safti FE-N, Mohammed S. Light and electron microscopic studies of chronic renal failure using an adenine rat model. Menoufia Med J. 2017;30(1):271.

[32] Toubeau G, Nonclercq D, Zanen J, et al. Distribution of epidermal growth factor in the kidneys of rats exposed to amikacin. Kidney Int. 1991;40(4):691–699.

[33] Cuzzocrea S, Mazzon E, Dugo L, et al. A role for superoxide in gentamicin-mediated nephropathy in rats. Eur J Pharmacol. 2002;450(1):67–76.

[34] Quiros Y, Vicente-Vicente L, Morales AI, et al. An integrative overview on the mechanisms underlying the renal tubular cytotoxicity of gentamicin. Toxicol Sci. 2011;119(2):245–256.

[35] Aldahmash BA, El-Nagar DM, Ibrahim KE. Reno-protective effects of propolis on gentamicin-induced acute renal toxicity in swiss albino mice. Nefrologia [Internet]. 2016;36(6):643–652. .

[36] Sadek E, Salama N, Ismail D, et al. Histological study on the protective effect of endogenous stem-cell mobilization in Adriamycin-induced chronic nephropathy in rats. J Microsc Ultrastruct. 2015;4(3):133.

[37] Bledsoe G, Shen B, Yao YY, et al. Role of tissue kallikrein in prevention and recovery of gentamicin-induced renal injury. Toxicol Sci. 2008;102(2):433–443.

[38] Farris AB, Colvin RB. Renal interstitial fibrosis: mechanisms and evaluation. Curr Opin Nephrol Hypertens. 2012;21(3):289–300.

[39] Suh SH, Lee KE, Park JW, et al. Antiapoptotic effect of paricalcitol in gentamicin-induced kidney injury. Korean J Physiol Pharmacol. 2013;17(5):435–440.

[40] Oliver L, Vallette FM. The role of caspases in cell death and differentiation. Drug Resist Updat. 2005;8 (3):163–170.

[41] Stojiljkovic N, Stoiljkovic M, Randjelovic P, et al. Cytoprotective effect of vitamin C against gentamicin-induced acute kidney injury in rats. Exp Toxicol Pathol [Internet]. 2012;64(1–2):69–74. .

[42] Abdelsameea AA, Mohamed AM, Amer MG, et al. Cilostazol attenuates gentamicin-induced nephrotoxicity in rats. Exp Toxicol Pathol. 2016;68 (4):247–253.

[43] Kohn S, Fradis M, Ben-David J, et al. Nephrotoxicity of combined treatment with cisplatin and gentamicin in the guinea pig: glomerular injury findings. Ultrastruct Pathol. 2002;26(6):371–382.

[44] Mahmoud YI. Kiwi fruit (Actinidia deliciosa) ameliorates gentamicin-induced nephrotoxicity in albino mice via the activation of Nrf2 and the inhibition of NF-κB (Kiwi & gentamicin-induced nephrotoxicity). Biomed Pharmacother [[Internet]]. 2017;94:206–218.

[45] Wakabayashi T. Megamitochondria formation - physiology and pathology. J Cell Mol Med. 2002;6 (4):497–538.

[46] Zaidi SK, Jafri MA, Tabrez S, et al. Reno-protective effect of garlic extract against immobilization stress induced changes in rats. Asian Pac J Trop Biomed [Internet]. 2015;5(5):364–369. .

[47] Gedik N, Kabasakal L, Sehirli O, et al. Long-term administration of aqueous garlic extract (AGE) alleviates liver fibrosis and oxidative damage induced by biliary obstruction in rats. Life Sci. 2005;76 (22):2593–2606.

[48] Hodge G, Hodge S, Han P. Allium sativum (garlic) suppresses leukocyte inflammatory cytokine production in vitro: potential therapeutic use in the treatment of inflammatory bowel disease. Cytometry. 2002;48(4):209–215.

[49] Hossain MA, Akanda MR, Mostofa M, et al. Therapeutic competence of dried garlic powder (Allium sativum) on biochemical parameters in lead (Pb) exposed broiler chickens. J Adv Vet Anim Res. 2014;1(4):189–195.

[50] Galal HM, Abd El-Rady NM. Aqueous garlic extract supresses experimental gentamicin induced renal pathophysiology mediated by oxidative stress, inflammation and Kim-1. Pathophysiology. 2019;26(3–4):271–279.

[51] Seckiner I, Bayrak O, Can M, et al. Garlic supplemented diet attenuates gentamicin nephrotoxicity in rats. Int Braz J Urol. 2014;40(4):562–567.